Geophys. J. R. astr. Soc. (1977) **51**, 91–119

A magnetotelluric and magnetovariational study of the Gregory Rift Valley, Kenya

D. Rooney and V. R. S. Hutton *Department of Geophysics, University of Edinburgh, James Clerk Maxwell Building, Mayfield Road, Edinburgh EH9 3JZ*

Received 1977 March 1; in original form 1976 November 24

Summary. Magnetotelluric measurements made at 10 locations in and around the Kenyan Rift Valley in 1973–74 have been processed to yield single station induction vectors and magnetotelluric principal impedances. Following a brief description of the field work and the data processing procedure, the results are presented and subjected to both qualitative and quantitative interpretations. The induction vector results indicate a concentration of current below the rift valley. Since the maximum impedances are along the rift for sites within the valley but at right angles to the rift outside it, the apparent resistivity results are qualitatively consistent with the existence of a good conductor there. Within the rift maximum apparent resistivities lie between 2 and 20 Ω m. The persistence of small induction responses and low apparent resistivities down to the shortest periods at which measurements were made suggests that the conductor lies at very shallow depths below the rift. The quantitative interpretation of the magnetotelluric results is given in terms of one- and two-dimensional conductivity models. It is shown that the data require the presence of conductive material at a depth less than 8 km below the rift floor but that the required thickness of this upper crustal conductor (> 5 km) is too great to be explained in terms of a conductive infill of the rift. The favoured explanation is in terms of high temperatures and water saturation of the crust under the rift. To satisfy the long-period data, conductive material is also required at depths of greater than 30 km, corresponding unambiguously to the upper mantle below the rift. Because of the obscuring effect of the crustal conductor, the depth to the top of and the thickness of the upper mantle conductor cannot be resolved.

1 Introduction

The East African rift system has attracted the attention of geologists and geophysicists over many years. During the past decade in particular, the apparent connection between certain continental rifts – such as that in East Africa – and the oceanic ridge system has raised questions of major tectonic significance (Baker, Mohr & Williams 1972; Fairhead & Girdler

1972; Milanovsky 1972; O'Connell 1972). In discussions of the results of the most recent geophysical studies in East Africa, the controversy continues as to whether or not the rifting in Kenya can be regarded as the first stage of continental break-up (Fairhead 1976; Long & Backhouse 1976; Scholtz, Koczyski & Hutchins 1976). Thus any further insight into the physical properties of the mantle and crust in the rift zone is of interest. While the electrical models and geophysical conclusions of previous electromagnetic induction work in the region (Banks & Ottey 1974; Beamish 1976) were strongly dependent upon the results of previous gravity and seismic investigations, the conductivity models discussed in this paper are based upon magnetotelluric observations alone, and are quite independent of other geophysical studies. It will be shown that in the strongly 'two-dimensional' region in which the project was undertaken, the magnetotelluric technique has provided more precise information than has been possible previously, about both the lateral and vertical extents of the conductor below the rift. The rift data are found to be consistent with a conductivity model similar to that obtained in magnetotelluric studies in Ethiopia (Berktold 1974) and Iceland (Hermance 1973) but before positive support can be given to one or other of the conflicting hypotheses regarding continental rifts, further magnetotelluric traverses of the rift system will be necessary at other latitudes.

2 The magnetotelluric method

The magnetotelluric technique for probing the electrical conductivity structure of the earth's crust and mantle was first presented in a practical form by Cagniard (1953). It involves the simultaneous measurement of the natural time variations of the earth's horizontal magnetic field, H and the orthogonal electric field E at the earth's surface. A response parameter, called the apparent resistivity ρ_a because of its direct relation to the actual resistivity in a homogeneous conductor, is determined over a range of frequencies. On the assumption that the conductivity is a function of depth only and that the external field configuration is known, curves of ρ_a versus frequency ω where

$$\rho_a = \frac{1}{\mu\omega}\left|\frac{E_x}{H_y}\right|^2 = \frac{1}{\mu\omega}\left|\frac{E_y}{H_x}\right|^2$$

can be used to infer the conductivity distribution at a single station to depths greater than 700 km. Here E_x and E_y are the amplitudes of the orthogonal components of the horizontal electric field and H_x and H_y of orthogonal components of the magnetic field at the earth's surface. It has however been found that at most locations ρ_a is dependent on the orientation of the telluric lines and that the assumptions of the classical Cagniard approach are seldom realized. Curves of maximum and minimum apparent resistivity versus frequency are frequently quite dissimilar in form and prior to the 1970's the ambiguity in interpretation of such results delayed the general acceptance of the magnetotelluric method as an important tool for probing the earth's interior. As the observed conductivity anisotropy is generally much larger than that found in laboratory measurements of rock conductivity it would appear that most cases of magnetotelluric anisotropy arise from lateral variations in conductivity (Dowling 1970; Porstendorfer 1975). However, a study of the general properties of two- and three-dimensional conductivity models indicates that the results of many magnetotelluric projects can be fitted by two-dimensional structures (Sims & Bostick 1969). With the introduction of practical two-dimensional modelling techniques (e.g. Jones & Price 1970; Coggon 1971; Reddy & Rankin 1972; Vozoff 1972) it has now become possible to obtain physical insight into the behaviour of apparent resistivity curves in the presence of lateral conductivity inhomogeneities. A schematic illustration of the effect of a vertical

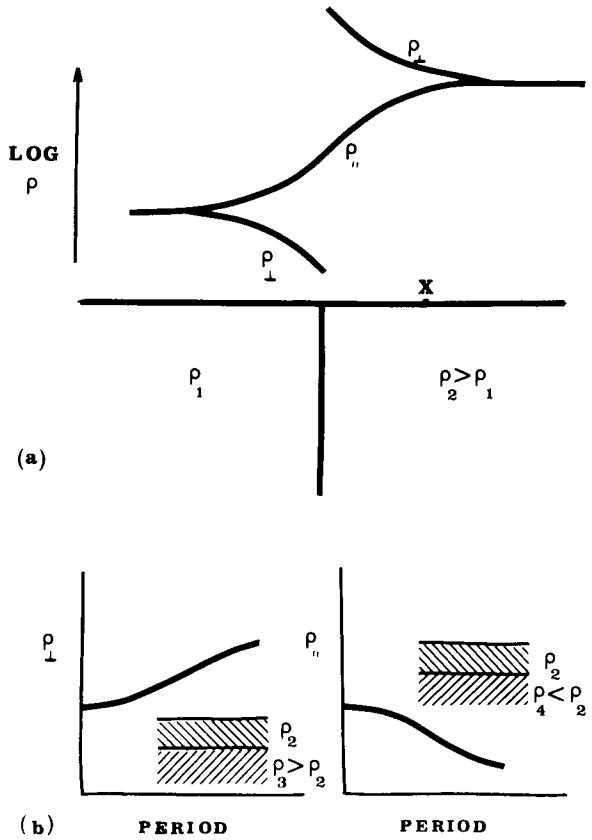

Figure 1. (a) Schematic illustration of the effect of a vertical discontinuity on the apparent resistivity in directions parallel and perpendicular to the strike. (b) Schematic illustrations of the frequency dependence of $\rho_{\parallel}$ and $\rho_{\perp}$ at a site X near a vertical discontinuity with corresponding Cagniard one-dimensional interpretations.

discontinuity on the apparent resistivities parallel and perpendicular – $\rho_{\parallel}$ and $\rho_{\perp}$ – to the strike of the discontinuity is given in Fig. 1(a) and the misleading interpretations which would result from a Cagniard one-dimensional interpretation of either ρ_{max} or ρ_{min} at a station X near the discontinuity is given in Fig. 1(b). It thus follows that no meaningful interpretation of anisotropic M–T data is possible from an isolated station. If however the form of the actual conductivity structure can be determined – for example by use of the 'induction arrow' or 'Fourier amplitude contour' presentations of the complementary technique of geomagnetic deep sounding, (GDS) (Gough 1973; Banks 1973) – then, with care, quantitative deductions about the conductivity structure are possible provided that M–T soundings are made at a series of sites across the anomalous structure (Reitmayr 1975; Kurtz & Garland 1976). As $\rho_{\parallel}$ is more closely related to the actual resistivities involved $\rho_{\parallel}$ values should be used for one-dimensional interpretations. On the resistive side of the anomaly, this corresponds to ρ_{min}, the minimum measured resistivity which, because of signal-to-noise considerations, cannot easily be estimated with great precision.

The magnetotelluric traverse in Kenya was undertaken in the same region as that in which Banks & Ottey (1974) and more recently Beamish (1976) have undertaken GDS measurements. The two-dimensional inductive behaviour of the region was thus known from their data. Their studies also indicated the existence of a good conductor directly beneath the rift

floor and another to the east of the main rift, but there was considerable ambiguity concerning the depth, thickness and conductivity of these conductors. As knowledge of these parameters beneath large-scale rift zones is of paramount importance to the understanding of the physical, chemical and tectonic processes responsible for the evolution of the earth's crust and mantle, a magnetotelluric traverse of this region was clearly desirable.

3 The fieldwork

Following the procedure adopted in some earlier studies (Caner & Auld 1968; Neinaber, Auld & Dosso 1973) two overlapping systems (Hutton 1976, Fig. 13) were employed so that natural magnetic signals whose amplitudes are strongly dependent on frequency could be detected over a wide period range. In one system, a three-component EDA fluxgate magnetometer built to the design of Trigg, Serson & Camfield (1970) was used to record variations of period greater than 200 s. Its output and that from an L-shaped array of three lead sheet electrodes were passed, prior to recording, through a low-pass filter with a cut-off period of 200 s. In view of the time required to obtain useful long-period data, variations of periods up to 24 hr were obtained at only two sites. The main effort was expended in

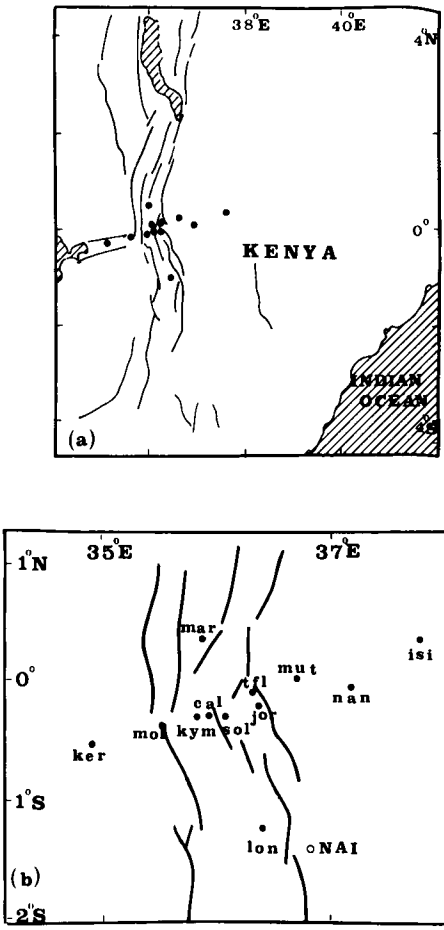

Figure 2. Maps showing (a) the geographical location of the observational sites and (b) their location in relation to the major faults of the Gregory Rift.

Table 1. Fieldwork location and observational bandwidth.

Station name	Geographic coordinates Long.	Lat.	Period range of observations
Isiolo (ISI)	37.62° E	0.36° N	10–1000 s
Kampi Ya Moto (KYM)	35.98° E	0.14° S	(a) 200 s – d.c. (b) 10–1000 s
Kericho (KER)	35.23° E	0.36° S	10–1000 s
Longonot (LON)	36.50° E	1.04° S	(a) 200 s – d.c. (b) 10–1000 s
McCall's Siding (CAL)	36.00° E	0.13° S	•
Marigat (MAR)	35.98° E	0.46° N	10–1000 s
Molo (MOL)	35.70° E	0.23° S	10–1000 s
Mutara (MUT)	36.68° E	0.13° N	10–1000 s
Nanyuki (NAN)	37.05° E	0.00°	10–1000 s
O1 Joro Orok (JOR)	36.40° E	0.06° S	10–1000 s
Solai (SOL)	36.08° E	0.10° S	10–1000 s
Thomson's Falls (TFL)	36.41° E	0.04° N	•

* Observations at these sites in the 10–1000 s period range had to be discontinued as a result of mains interference.

acquiring good-quality data in the period range 10–1000 s at as many sites as time and finances would permit. The very sensitive torque magnetometers designed by Jolivet (1966) and modified by Albouy, Godivier & Perichon (1971) were used for this short-period system. Adequate sensitivity for detection of the short-period telluric variations was obtained by inserting low-noise pre-amplifiers in the telluric lines prior to filtering and further amplification.

A detailed description of the instrumentation, its deployment in the field, methods of field and laboratory calibration and a discussion of different noise effects encountered during the field operation are given in Rooney (1976).

Observations were made at 12 sites on an approximately equatorial traverse of the Gregory Rift and at an additional two sites along the rift axis – Fig. 2. The coordinates of these sites and comments about the observations made are given in Table 1.

Simultaneous observation of the H and D magnetic elements was undertaken at Isiolo and Nairobi to provide an estimate of the horizontal dimensions of the inducing field in the period range 10–300 s. For data with coherence greater than 0.9, the ratio of H_{NAI} to H_{ISI} was found to vary between 0.9 and 1.1 irrespective of the time of day. An example of the results of the comparison of one of the events examined is given in Fig. 3. The effect of source field dimensions on the magnetotelluric analysis was thus assumed to be insignificant.

4 Data analysis

4.1 SINGLE EVENTS

Fron the records obtained at each site, several data sections or 'events' of duration approximately 130 min (short-period system) and 200 hr (long-period system) were selected visually for digitizing. The criterion for event selection was the presence of a high degree of activity on the D magnetic component – This is necessary on account of the typically strong north–south polarization of the horizontal magnetic fields at low latitudes. After editing, scaling and interpolation, the linear trend was removed from each time series. It was then pre-whitened, tapered 10 per cent at each end with a Tukey cosine bell window and augmented to 2048 points by the addition of zeros. Power spectral estimates were obtained using the

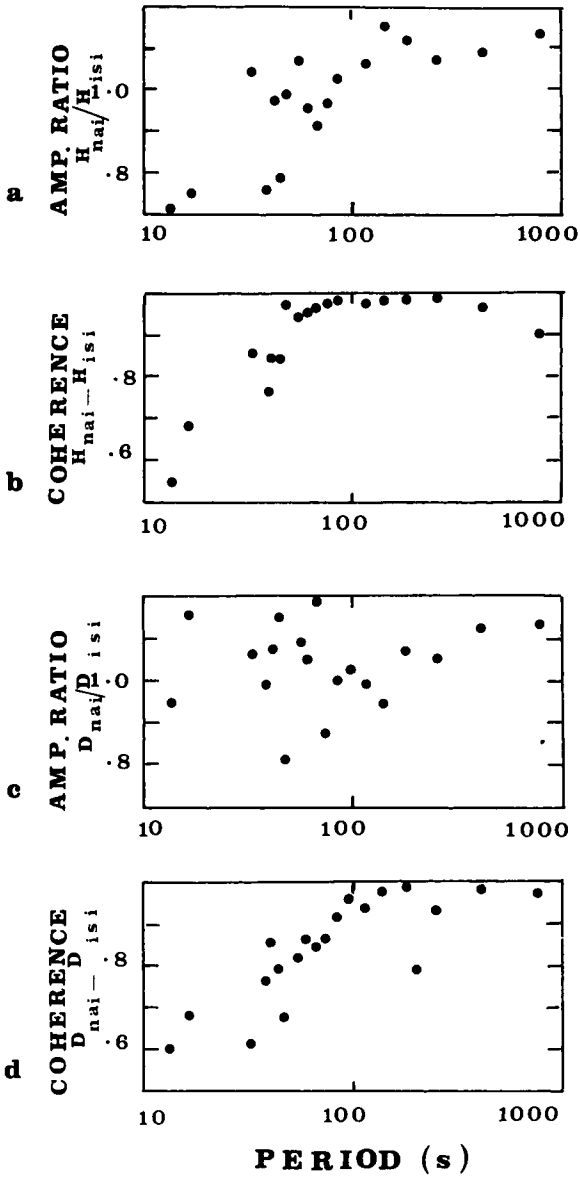

Figure 3. Comparison of simultaneous magnetic field observations at Nairobi and Isiolo 1200–1300, 1974 April 4 in the period range 10–1000 s. (a) Ratio of H amplitudes. (b) Coherence between H components. (c) Radio of D amplitudes. (d) Coherence between D components.

IBM SSP routine RHARM which implements the Cooley–Tukey algorithm. Auto and cross-spectral estimates were averaged over eight neighbouring frequencies except for the first and last which were averaged over four. The first smoothed estimate was not used in later interpretation on account of distortion by leakage effects and a correction (Kanasewich 1973, p. 179) was applied to the others to compensate for the effect of recording different components with different high-pass filters.

The smoothed power estimates of the two telluric and three magnetic components formed the basis from which the following parameters were then calculated:

(a) Polarization parameters of both the horizontal magnetic and telluric fields (Fowler, Kotick & Elliot 1967).

(b) Coherence between orthogonal magnetic and electric field components and, from them, the Cagniard apparent resistivities (Sims & Bostick 1969).

(c) Estimates of the tensor impedances using expressions of the form

$$Z_{xy} = (\langle H_x H_x^* \rangle \langle E_x H_y^* \rangle - \langle H_x H_y^* \rangle \langle E_x H_y^* \rangle)/(\langle H_x H_x^* \rangle \langle H_y H_y^* \rangle - \langle H_x H_y^* \rangle \langle H_y H_x^* \rangle)$$

where the terms in angular brackets represent averages of the auto and cross powers at a fixed trequency over a frequency band width (Sims, Bostick & Smith 1971).

(d) Transfer function estimates for the Z magnetic component using an expression similar to that for Z_{xy} but with H_z substituted for E_x. This least-squares estimator had been found in earlier studies (e.g. Banks & Ottey 1974) to produce reliable repeatable results even when the magnetic field was strongly polarized. Using the standard notation A and B for the complex vertical transfer function, 'real' and 'imaginary' induction arrows were determined with magnitudes

$$M_R = (A_R^2 + B_R^2)^{1/2} \text{ and } M_I = (A_I^2 + B_I^2)^{1/2} \quad (1)$$

and with angles θ_R and θ_I between their directions and the local geomagnetic meridian given by

$$\tan \theta_R = B_R/A_R \text{ and } \tan \theta_I = B_I/A_I \quad (2)$$

(e) The coherence between the measured vertical magnetic field Z_M and that predicted by the linear transfer function relation $Z(f) = \bar{A}(f) H_M(f) + \bar{B}(f) D_M(f)$ where $\bar{A}$ and $\bar{B}$ are estimates of A and B respectively. This so-called 'predicted' coherency provides a measure of the contamination by random noise in the transfer function relationship (Kurtz & Garland 1976). Predicted coherences were similarly determined for each of the telluric components.

(f) The azimuth of the major principal impedance axis, the principal impedance estimates and the principal apparent resistivities, all as defined by Swift (1967) for two-dimensional structures, and

(g) The skew factor, a measure of two-dimensionality, and the ellipticity factor – the ratio of the minor to major axis of the polarization ellipse (Swift 1967) which is a measure of the degree of polarization.

This procedure for single-event analysis and a discussion of the sources of noise and systematic errors in the Kenyan data – particularly those which arose due to source field polarization effects – are discussed in full by Rooney (1976).

4.2 EVENT AVERAGING THE ERROR ESTIMATION

The computer program written for the single-event analysis incorporated routines for printing out all the parameters and for plotting most of them. In this way the characteristics of each event could be examined prior to the sequence of operations performed for event averaging. Transfer functions and tensor impedances were accepted for this additional processing only if they satisfied the following two criteria, namely:

(a) all relevant components possessed a power level five times that of the random noise power,

(b) the predicted coherence was greater than 0.7 for measured Z and was greater than 0.9 for one of the measured telluric components.

Acceptable transfer functions and tensor impedances were then averaged over the events and over period bands equispaced on a log (period) scale in such a way as to provide 10 estimates per decade. The number of smoothed single-station estimates, N_s, contributing to each final average was recorded. Confidence limits were determined from the variances of the transfer functions and tensor impedances, assuming they are normally distributed; as this assumption leads to larger error bars than would result from the assumption of a log-normal distribution (Bentley 1973), these confidence limits, and the error bars – representing 80 per cent confidence limits – based on them, can be regarded as conservatively estimated.

Averaged real and imaginary induction arrows were obtained using equations (1) and (2) with the averaged transfer function estimates. Maximum and minimum response arrows were also calculated by rotating the measuring axes into directions which maximized and minimized the responses. As shown by Banks & Ottey (1974) this maximum and minimum

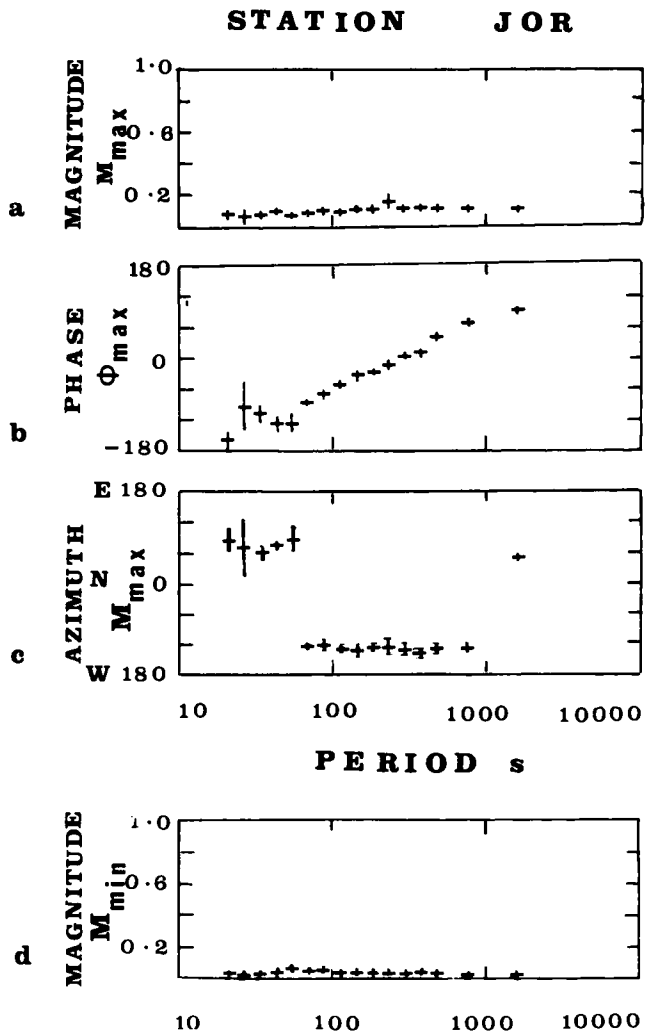

Figure 4. Induction vectors at O1 Joro Orok (JOR). (a) Magnitude of maximum response function M_{max} versus period. (b) Phase of maximum response function ϕ_{max} versus period. (c) Azimuth of maximum response function versus period. (d) Magnitude of minimum response function M_{min} versus period.

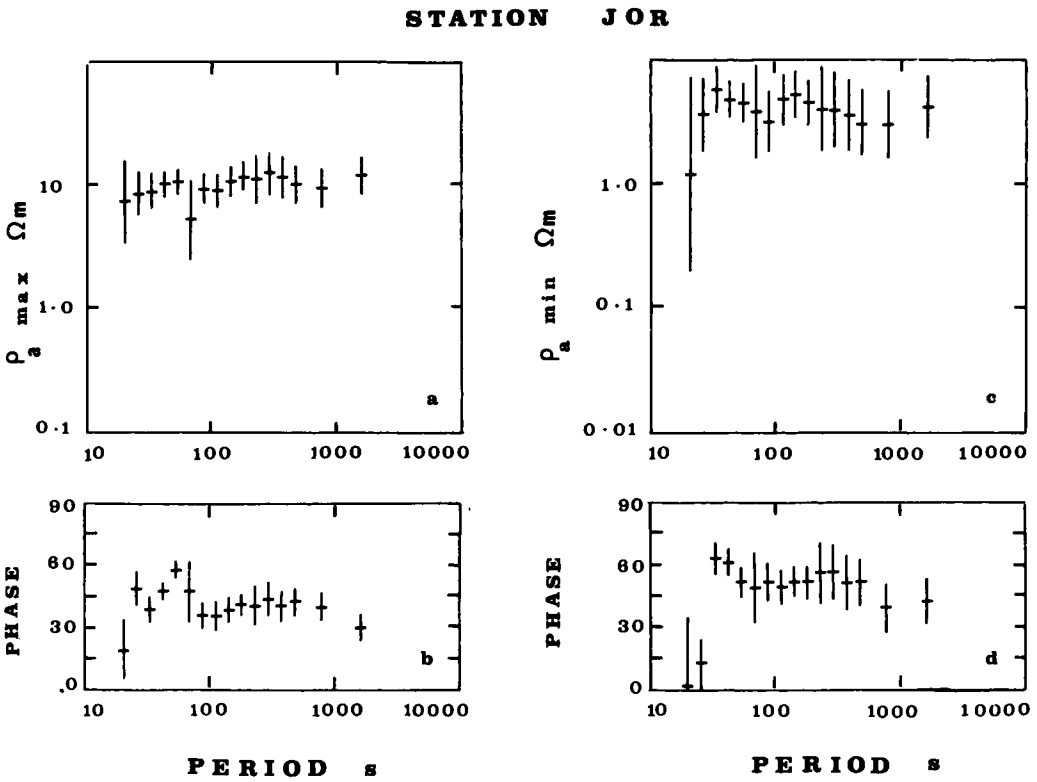

Figure 5. The period dependence of: (a) maximum apparent resistivity and, (b) phase of ρ_{max} at JOR. (c) Minimum apparent resistivity and, (d) phase of ρ_{min} at JOR.

response function technique leads to a simple interpretation in the two-dimensional situation for which the minimum response should be zero and the azimuth of the maximum response should be perpendicular to the strike of the conductor. For these parameters, and also for the azimuth of the principal impedance, error bars were calculated from their functional relationships with transfer functions and tensor impedances using the expression for propagation of errors. Principal impedances and phases and their errors and also the skew factors were re-calculated as for the single event analysis but using the averaged tensor impedance values. Lognormal statistics were adopted in calculating principal apparent resistivities and their errors, following the treatment by Bentley (1973).

Computer plotting routines were also included in this computer program for the presentation of all the averaged parameters evaluated. To illustrate the procedure, the event averaged results for the station JOR are presented in full in Figs 4–6. For the other stations, only the results referred to in the discussion are given in the subsequent figures.

5 Results

5.1 INTRODUCTION

The results of this study are considered in the following manner:

(a) The event-averaged results for the Rift Valley station of JOR which are presented in full form the basis for the limited interpretation which can be made from such single-station data.

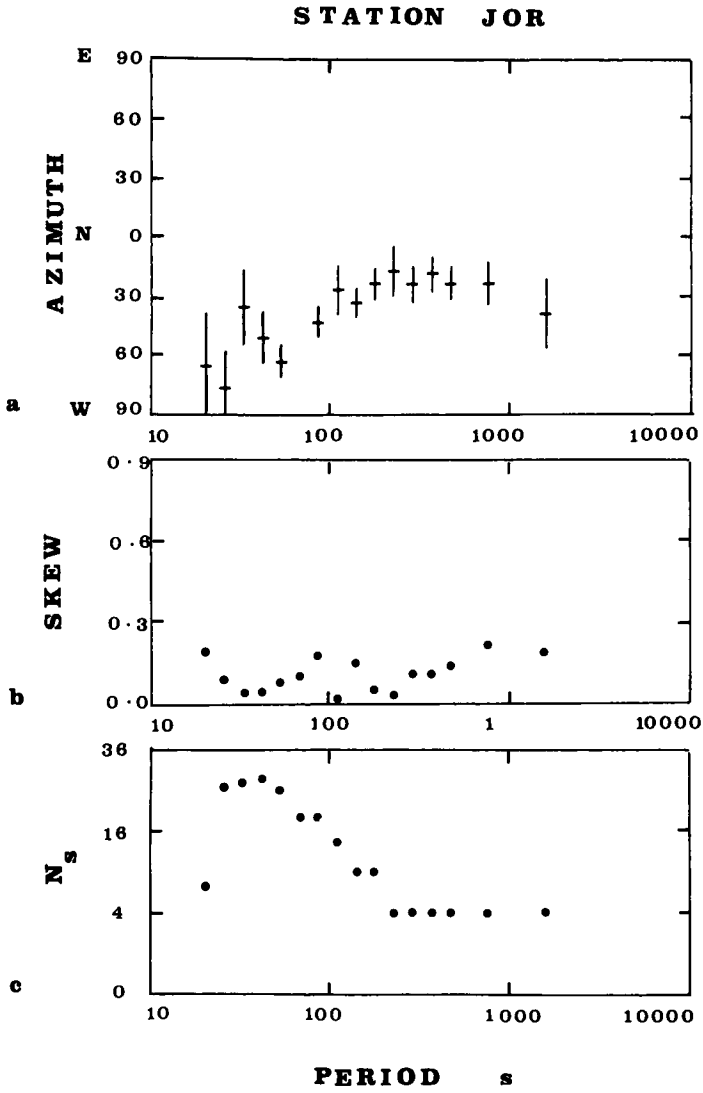

Figure 6. The period dependence of: (a) azimuth of ρ_{max}, (b) $M-T$ skew factor at JOR. (c) Number of single station estimates, N_S.

(b) The apparent resistivity versus period curves and the azimuth of the major axis are given *for four stations* on the equatorial traverse – Fig. 7. The marked difference in these parameters between stations in the Rift and those outside it is discussed.

(c) The principal impedances and maximum and minimum response functions *for all stations* are plotted in Fig. 8(a) and (b) for periods of 30 and 1000s. A qualitative interpretation of the rift valley anomaly is based on these data.

(d) A one-dimensional interpretation (a) using Schmucker's (1970, 1973) inversion technique and (b) applying two-layer Cagniard master curves is given for the rift valley station JOR for which the response estimates are well determined, have low anisotropy at short periods and have a low skew factor at all periods. This is complemented by discussions of the results of two-dimensional modelling using the programs developed by Pascoe & Jones (1971) and of the geophysical significance of the interpretation.

5.2 RESULTS FOR OL JORO OROK

The variations with period of the maximum response function parameters – magnitude, phase and azimuth – and of the magnitude of the minimum response function are given in Fig. 4(a)–(d) for Ol Joro Orok (JOR) which is situated on the eastern escarpment of the rift valley. Although the maximum response amplitude is less than 0.1 the signal-to-noise ratio is high. Thus the strong two-dimensional behaviour of the response functions, indicated by the negligible amplitude of the minimum response function at all periods, is still observable at this station. The phase of the maximum response increases continuously with period from less than $-120°$ at 30 s to $+90°$ at 1500 s and as it passes through $-90°$, the azimuth of the maximum response arrow changes discontinuously from 90° E of N to 120° W of N.

The maximum and minimum apparent resistivities and phases are plotted against period in Fig. 5(a) and (b) and the period dependences of (i) the azimuth of the maximum apparent resistivity, (ii) the skew factor and (iii) the number N_s are given in Fig. 6(a)–(c). With the exception of the skew factor, which indicates strong two-dimensionality at all periods at JOR and N_s, the data are presented and discussed in Section 5.3, along with similar results from other stations.

5.3 THE MAGNETOTELLURIC RESULTS FROM STATIONS ON THE EQUATORIAL TRAVERSE

The magnetotelluric results for MOL and JOR which lie on the escarpments of the rift valley and for KER and MUT which are approximately 50 km distant from it are presented in Fig. 7, the location of these stations relative to the main rift faults being given in Fig. 7(i). The apparent resistivity curves, Fig. 7(a)–(d), show the period dependence of the maximum and minimum resistivities after a mathematical rotation of the measuring axes and the polar diagrams, Fig. 7(e)–(h), give the period dependence of the azimuths of the major resistivity axes at the four stations. There are several features of interest in these results. The magnetotelluric responses at MOL and JOR are similar to each other – they are also similar to those measured at other stations in the rift – but are dramatically different from those recorded at stations outside the rift, represented here by KER and MUT. For example, the maximum resistivities at the rift stations MOL and JOR are more than one order of magnitude smaller than those at stations KER and MUT outside the rift. Secondly, the degree of anisotropy is smaller at MOL and JOR than at stations outside the rift by a factor of about three. Thirdly, the direction of the major resistivity axis at stations outside the rift is approximately perpendicular to the main rift faults while at stations inside the rift and on its escarpments, the major axis is nearly parallel to the rift axis. As these results are presented again but in a different form in Fig. 8 together with data from all the observing sites, discussion of their significance is given later.

5.4 THE MAXIMUM RESPONSE FUNCTIONS AND PRINCIPAL IMPEDANCES

5.4.1 Results

The behaviour of the induction arrows and major characteristic impedances is illustrated in Fig. 8(a)–(d) for all stations and for the periods of 30 and 1000 s respectively. Similar results have been obtained for intermediated periods.

Considering first the stations on the line of traverse, the most obvious feature of the principal impedance diagrams is the large difference in amplitude of the major impedances at both periods between stations outside the rift valley and stations within the rift and on its

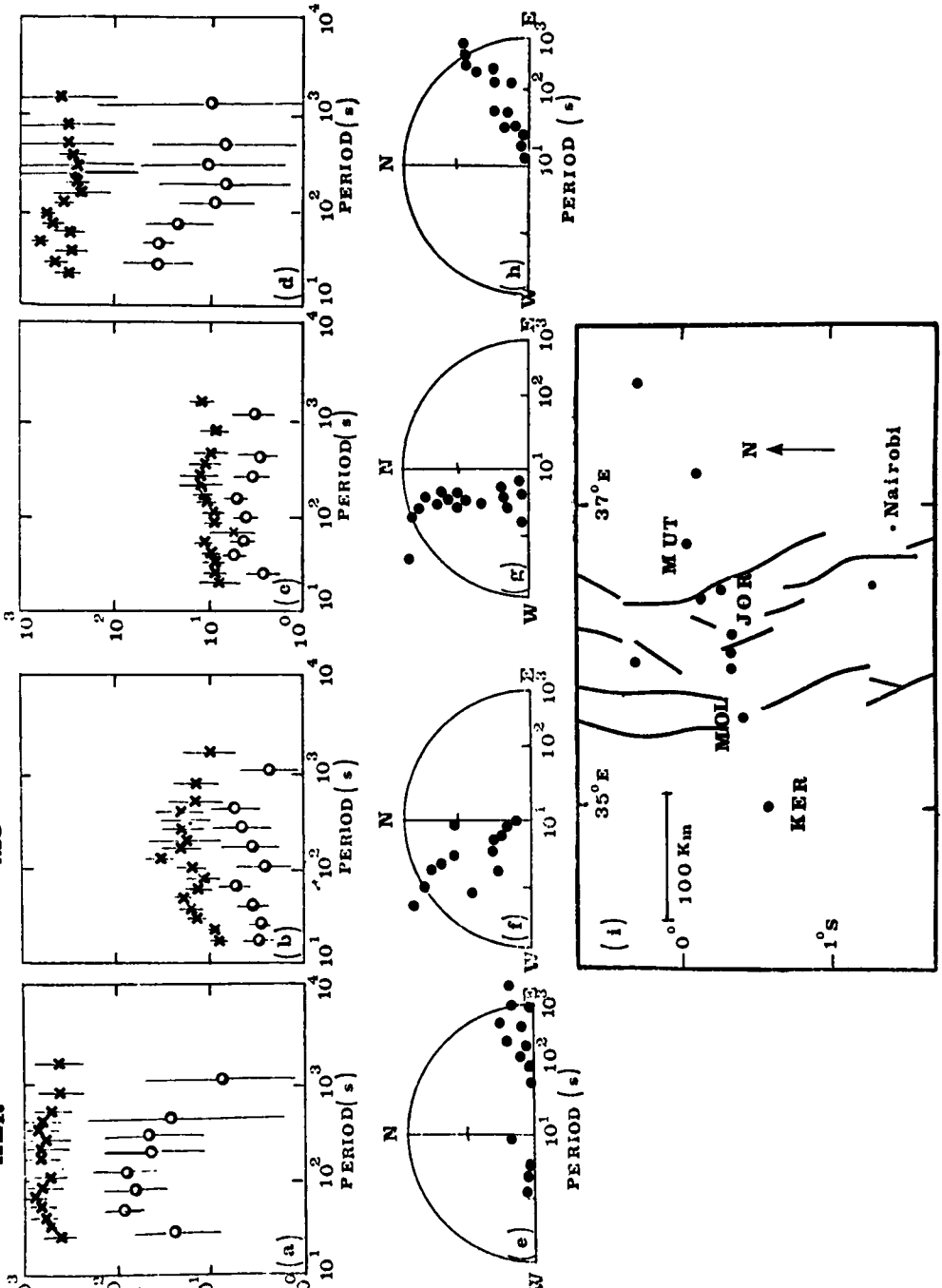

Figure 7. The variation of maximum and minimum apparent resistivity with period: (a) KER, (b) MOL, (c) JOR and (d) MUT. The variation with period of the azimuth of the major resistivity axis: (e) KER, (f) MOL, (g) JOR and (h), MUT, (i) the location of KER, MOL, JOR and MUT relative to the major faults of the rift.

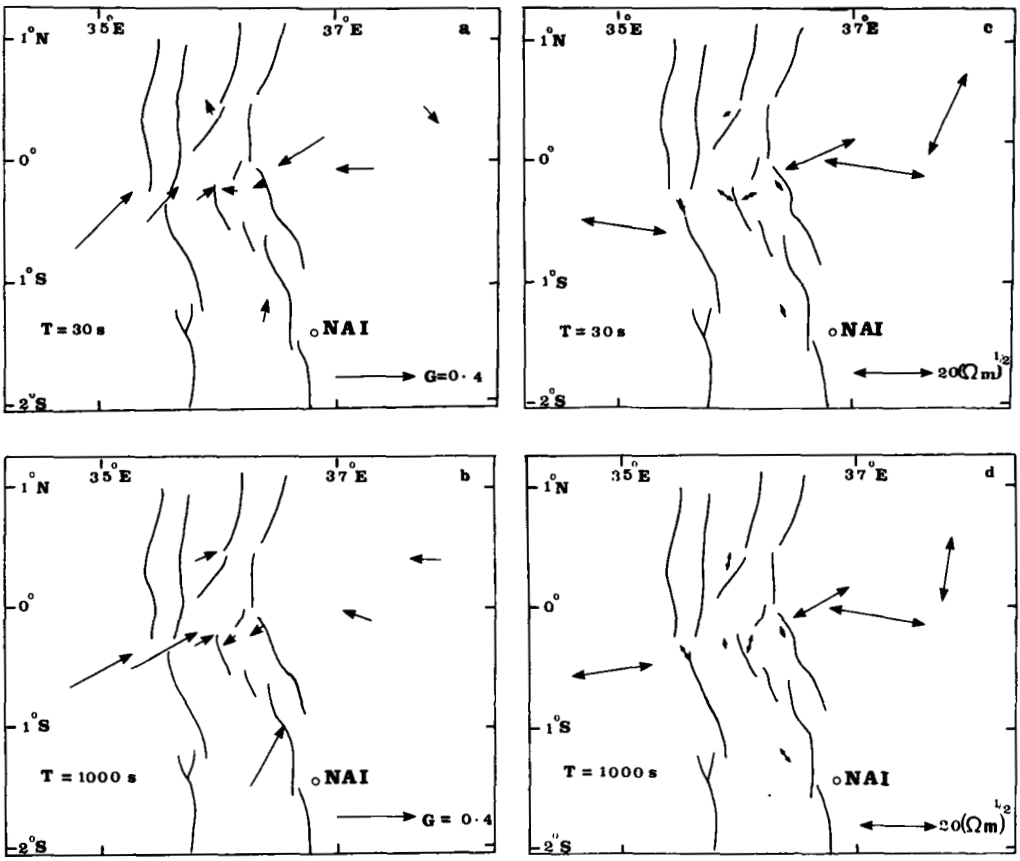

Figure 8. Maximum response arrows across and along the Gregory Rift Valley, Kenya: (a) T = 30 s. (b) T = 1000 s.
Azimuths and amplitudes of the major characteristic impedances across and along the Gregory Rift Valley, Kenya: (c) T = 30 s. (d) T = 1000 s.

shoulder. The amplitude of the minimum apparent resistivities at the non-rift station tends also to be larger than the maximum apparent resistivities within the rift, especially for the shorter periods. The azimuth of the major impedance axis shows very little change with period at all sites except SOL where all M–T parameters show very great scatter and are thus not considered further in this discussion. For all other sites which have low maximum resistivities, the major resistivity axes are approximately parallel to the strike of the main rift faults; for KER and MUT which have large maximum apparent resistivities and lie outside the rift, the major impedance axes are directed approximately perpendicular to the rift.

Maximum response arrows at stations along the traverse line from KER in the west to MUT in the east are very accurately parallel to each other and perpendicular to the strike of the rift for periods of 100 s and above. They are thus oriented approximately parallel to the major impedance axes at KER and MUT outside the rift and perpendicular to the major impedance axes at stations within the main rift faults. Further east at NAN, the maximum response arrow is again parallel to the major impedance axis but the axes of both these responses show a difference in orientation of about 40° from the other stations in the traverse. At KER, MOL, KYM, JOR, MUT and NAN, the ratios of the minimum to maximum induction response and the M–T skew factor indicate that all these stations are

associated with a geoelectric structure which is strongly two-dimensional. At ISI, on the other hand, skew values are high and neither induction response nor impedance behaviour can be interpreted in terms of a simple two-dimensional model.

5.4.2 Qualitative interpretation

For a two-dimensional situation, a qualitative interpretation of induction response data can be based on the following considerations:

(a) maximum response arrows are normal to and point in the direction of current concentrations, and
(b) the magnitude of the maximum response is proportional to the intensity of anomalous current concentrations. This intensity will depend on the steepness of the conductivity interfaces and the conductivity contrast across the interface.

From the reversal of the induction response arrows, it is apparent that there is a concentrated current within the region of the rift valley, flowing approximately parallel to the strike of the main rift faults. As the predominant external current system in this region has an east–west orientation, the current concentration indicated by the response functions must be associated with a good conductor beneath the rift valley. The variation in amplitude of the maximum response functions along the traverse suggests that the western edge of the conductor is between KER and MOL and the eastern edge in the region of MUT.

As the maximum response amplitudes are smaller on the eastern flank of the rift than on the western flank, the volume integrated rate of change of conductivity must be more gradual towards the east. This could arise as a result of (a) a smaller conductivity contrast at the eastern edge of the conductor, (b) a conductor–resistor interface which has a more gradual slope to the east, or (c) the presence of a second conductor beneath the area to the east of the rift as suggested by Banks & Ottey (1974) and Beamish (1976) to explain their GDS observations.

The *M–T* impedances provide independent evidence of the lateral extent of the rift conductor and the consistently low ρ_a values at all stations within the rift valley are strong evidence for the existence of a very good conductor underlying it. In an ideal two-dimensional case, as discussed in Section 2, stations positioned near a conductor–resistor interface have the maximum resistivity axis oriented parallel to the interface if the station is on the conductive side of the contact and perpendicular to the interface if the station lies over the resistor. The orientations of the major impedance axes measured at stations on the traverse thus indicate that the western edge of the conductor is between MOL and KER and the eastern edge between MUT and JOR.

Measurements at the stations MAR and LON, north and south respectively of the main traverse and within the rift valley display some interesting features. The low apparent resistivities at LON suggest that the station lies on the conductor, but since the skew factor is high, the conductor cannot have a simple two-dimensional character in this region. This can also be deduced from the fact that the maximum response arrow is not perpendicular to the major impedance axis. The increase in amplitude of the maximum response arrow from 0.15 at 30 s to 0.45 at 1000 s could result from a current concentration and/or the presence of the southern edge of the rift conductor in the vicinity of LON.

The apparent resistivities at MAR are the smallest obtained in this *M–T* project, both maximum and minimum resistivities being less than 4 Ω m at short periods. Since MAR lies between Lakes Barringo and Hannington on lake sediments, such low resistivities are not unexpected. The direction of the major impedance axis at this station corresponds, at all periods, with the direction of strike of the major rift faults in the area – a direction which

bears an angle of 40° to that of the strike at 0° latitude. At long periods, the maximum resistivities, corresponding to the E polarization case, appear to increase to a value of about 15 Ωm, i.e. approximately the same as the maximum resistivities for other stations situated over the rift conductor. The main rift conductor thus appears to extend northwards beyond MAR; the small induction arrows at MAR provide supporting evidence for this deduction.

At NAN, the character of the induction arrows is significantly different from that at any of the other stations on the traverse, especially at long periods. While the ratio of the minimum to maximum response is consistent with the existence of a two-dimensional structure at all periods, the orientation of the induction arrow shows a significant difference in direction (~40°) at NAN to the direction at the six stations on the traverse to the west of NAN. As for the other traverse stations on the flanks of the rift, the major impedance axes and the maximum induction arrows at NAN are strictly parallel to each other. The M–T anisotropy at NAN is, however, much greater than at any of the other stations in the project, with the ratio of the maximum to minimum resistivities being more than 500 to 1.

6 Conclusions from the qualitative interpretation of the data

The advantages of recording three components of the magnetic field along with two telluric components and the subsequent application of the techniques of both geomagnetic deep sounding and the magnetotelluric method is clearly shown by this study. The interpretation of the results of both techniques confirms the existence of a good electrical conductor coinciding with the main rift valley in Kenya. Its lateral extent is reasonably well defined by this qualitative examination of the data but deductions about the depth to the top of the conductor require the application of mathematical modelling techniques such as are described in the following sections. Data from Longonot (LON) are consistent with this station lying close to the southern edge of the conductor, a result which shows an interesting correlation with the southern termination of the regional gravity anomaly (Fairhead 1976). Between 0° and 5° S, seismologicai evidence (Knopoff & Schlue 1972) is consistent with the termination of partial melting under the rift and there is a change in the tectonic style of faulting (Fairhead & Girdler 1972). The implication of the 40° difference in orientation of the geoelectric structures affecting MUT and NAN, which are only 45 km apart, requires further consideration.

7 Theoretical considerations for mathematical modelling

7.1 INTRODUCTION

As satisfactory modelling techniques are available at present only for the treatment of one- and two-dimensional conductivity structures, a quantitative interpretation can only be made of M–T data which have pronounced one- or two-dimensional characteristics. In the latter case also, the assumptions of (a) a single regional two-dimensional geoelectric structure as opposed to several local two-dimensional structures and (b) a uniform inducing field are required. For the Kenyan data, the remarkable consistency of the maximum resistivity values and of the orientations of maximum resistivity axes at all stations within the rift and on its escarpments justifies the assumption of a single regional conductor. With respect to the source field, simultaneous measurements of horizontal magnetic variations of period 10–300 s at Nairobi and Isiolo, approximately 200 km apart, showed that the difference in amplitude was less than 10 per cent and the shortest spatial wavelengths thus of the order of 2000 km. As this value is very much greater than the depths associated with the M–T sounding, the assumption of source field uniformity is also applicable in this study.

Although the response parameters used in the subsequent interpretation have a strongly two-dimensional character, the possibility must be considered that this two-dimensional behaviour may be due to current channelling by the Gregory Rift conductor of currents induced over a very wide area in a three-dimensional geoelectric structure. The following argument shows that such a possibility seems unlikely. The existence of a highly conducting path – required to channel the large currents induced in the Indian Ocean into the rift conductor – seems to be improbable in the region to the east of the Kenyan rift since the sediments extend only 200–300 km inland and then a high-resistance barrier of about 200 km of metamorphic and igneous rocks is encountered. While a conductive path from the Indian Ocean through the Gulf of Aden and the Ethiopian rift is perhaps more probable, one would expect as a consequence of such current channelling that the coherence between the channelled current induced at large distances from the recording site and the local magnetic variations would be low. As the data interpreted here are derived from records showing a high coherence (>0.9) between electrical and magnetic components, it seems reasonable to assume that the contribution due to channelled currents is negligible.

7.2 SELECTION OF DATA FOR QUANTITATIVE INTERPRETATION

Because M–T responses are contaminated by the presence of lateral inhomogeneities located within approximately one skin depth of the measuring station, responses at stations located over a resistor usually appear more distorted than the corresponding responses for a station overlying a conductor. Even assuming a low value of 300 Ωm for the resistive basement in Kenya, responses at the shortest recording period of about 30 s will be affected by lateral conductivity changes within 50 km of the recording station. The usefulness of response data at stations on the resistor is also limited by simple instrumental and data processing considerations, since the apparent resistivity estimates least affected by lateral inhomogeneities at these stations are the $\rho_{\min}$ estimates. On account of the low signal-to-noise level on the telluric component along the minor impedance axis, these estimates tend to have much greater scatter than the corresponding $\rho_{\max}$ estimates and at the same time they are affected by systematic bias. More importantly, from the point of view of quantitative interpretation, the $\rho_{\min}$ estimates can show a considerable bias; it can be demonstrated that this bias is enhanced in the presence of strong source field polarizations (Rooney 1976).

For these reasons, the apparent resistivity curves obtained at stations off the rift conductor are more difficult to interpret quantitatively than those on the conductor and in this study they have been used only to indicate the lateral extent of the rift conductor – Section 5.4.2. The quantitative interpretation is thus based on the high quality data obtained at several of the rift conductor stations and is aimed at establishing the types of geophysically distinct models which are compatible with the M–T data. It is considered that an approach which aims at constraining the range of possible conductivity models and assigning approximate dimensions to the conductor is more satisfactory than one which attempts to model the data in some 'best fit' way using highly idealized conductivity models and two-dimensional modelling techniques which are not completely reliable.

The main emphasis in the following interpretation is thus placed on the results of the rift valley stations of JOR and MAR at which the good quality data with very low skew factors can be subjected to one-dimensional interpretations. Two-dimensional modelling techniques are then employed in a semi-quantitative way to show that the E polarization curves are very similar in shape and amplitude to one-dimensional curves and thus to strengthen the validity of the one-dimensional interpretation.

7.3 THE SOURCE FIELD DIMENSIONS

Price (1962) has shown that the relation between the orthogonal electrical and magnetic fields in the mth layer of conductivity σ_m is

$$\frac{E_x}{H_y} = \frac{-i\omega\mu}{\theta_m} \cdot \frac{A \exp(\theta_m z) + B \exp(-\theta_m z)}{A \exp(\theta_m z) - B \exp(-\theta_m z)}$$

where $\theta_m^2 = \upsilon^2 + i\omega\mu\sigma_m$ and $\upsilon^{-1} = 2\pi$ times the spatial wavenumber of the inducing field of frequency ω. The radio E/H is called the characteristic impedance Z. In general, the complete solutions of the basic diffusion equations can be very complex and are rarely used other than to calculate the effect on the interpretation of neglecting the source field distribution. It can however easily be shown that source fields can be regarded as horizontally uniform if the horizontal wavelength is very much greater than the depth of penetration δ in the earth where

$$\delta = 0.504\sqrt{T/\sigma}\,\text{km} \tag{3}$$

assuming units of seconds and siemens per metre for T and σ respectively.

It has been shown in Section 3 that for the period range 10–300 s this condition is satisfied in the Kenyan project. For longer periods it can also be assumed that υ equals zero since the project location was several degrees south of the electrojet region in which the spatial dimensions of the longer period variations might be significant (Hutton 1972).

7.4 QUANTITATIVE INTERPRETATION OF SINGLE-STATION $M-T$ DATA

The apparent resistivity ρ_a defined as

$$\rho_a = \frac{1}{\mu\omega}|Z(0)|^2 \text{ and} \tag{4}$$

introduced by Cagniard (1953) in his classical work is a parameter which has proved to be very useful in interpreting magnetotelluric data, because of its association with the actual resistivity in a homogeneous geoelectric structure. For a two-layered earth, a single family of master curves can be used to fit a plot of ρ_a versus T. While this standard curve-matching technique of M–T interpretation can be extended to three or more layers (Berdichevsky 1968) there are many independent parameters in a multi-layered master model. A very large number of sets of master curves is thus required to represent the full range of resistivity combinations. In this situation it is frequently simpler to employ a direct inversion method and to derive a satisfactory model directly from the data.

The method most commonly used to invert M–T data is the method of least-square error, several variations of which are discussed by Laird & Bostick (1970). Another method which is a very simple but effective scheme for inverting complex impedance estimates has been developed by Schmucker (1970). It requires reliable phase data such as has been obtained at some of the Kenyan rift valley stations.

In the two-layer case of a resistive surface layer overlying a conductive substratum, θ_1 may be approximated by the wavenumber υ in the top layer, and θ_2 may be replaced by $(1+i)\delta_2$ in the conductor where δ_2 is the skin depth defined by equation (3). Assuming also that the thickness h of the upper layer is small compared with the dimensions of the source field, i.e. $h\upsilon \ll 1$, then to a first approximation, it can be shown that

$$\frac{Z(0)}{i\omega\mu_0} = h + \frac{\delta_2}{2} - i\frac{\delta_2}{2}.$$

Replacing the left-hand expression by C, it follows that

$$\rho_2 = 2\omega\mu_2(\mathrm{Im}\{C\})^2 \tag{5}$$

and

$$h = \mathrm{Re}(C) + \mathrm{Im}(C). \tag{6}$$

Thus if impedance estimates have been determined above a multi-layered substratum, equations (5) and (6) can be applied to obtain for each frequency component the depth to the top and the resistivity, respectively, of a uniform substitute conductor. Such an interpretation is physically meaningful only when the phase of Z lies between $\pi/4$ and $\pi/2$. When h is positive, the multi-layered substratum may be replaced by a uniform conductor at depth h, as far as its response to one frequency is concerned.

For the case of a multi-layered earth, Weidelt (1972) has shown that $\mathrm{Re}(C)$ can be equated to the mean depth, h^*, of the in-phase eddy currents. Since a multi-layered conductor can be represented in its response at any frequency by a two-layered Schmucker model, equation (5) can be used to determine the resistivity, ρ_2, corresponding to the depth h^* at which current is concentrated, where

$$h^* = \mathrm{Re}(C) = h + \frac{\delta_2}{2}. \tag{7}$$

Thus a plot of the depth of current flow, h^*, versus resistivity ρ_2 of a uniform substitute conductor represents a good approximation to the actual resistivity distribution (Schmucker 1970).

7.5 QUANTITATIVE INTERPRETATION OF TWO-DIMENSIONAL $M-T$ DATA

It is frequently found in $M-T$ fieldwork that the telluric signals predominate in a certain direction resulting in anisotropic apparent resistivity versus period curves such as found at Kericho, Kenya – Fig. 7. In such cases, the field data can not be interpreted in terms of layered geoelectric structures but are indicative of lateral conductivity inhomogeneities. Mathematical problems arise in the case of three-dimensional structures, but if the structure has the same form for a distance of a few skin depths along its strike, the criterion of two-dimensionality is satisfied. The solution of the two-dimensional induction problem has been considered by several workers. It separates into two distinct modes – the E polarization or $\rho_\parallel$ mode in which the electric field is polarized parallel to the strike of the conductor and the H polarization or $\rho_\perp$ mode in which the magnetic field is polarized in this direction. Analytic solutions exist for only very special conductivity distributions, but for the general two-dimensional problem, various numerical methods are available (Jones & Price 1969; Madden & Swift 1969; Coggon 1971; Reddy & Rankin 1972) and they have been widely used in magnetotelluric interpretation. There is, however, considerable debate as to the acceptability of the numerical solutions.

A schematic illustration of the effect of a vertical discontinuity on $\rho_\parallel$ and $\rho_\perp$ is given in Fig. 1. Additional features of the two-dimensional situation become apparent when the measuring axes are rotated through an angle θ to yield maximum and minimum impedance values. These principal impedances can easily be shown to correspond to the impedances parallel and perpendicular to the strike of the conductor although not necessarily in that order and θ and $(\theta + 90)$ to the orientations of the principal axes, one of which must be in the direction of strike. For a strictly two-dimensional situation, the diagonal tensor elements $Z_{xx'}$ and $Z_{yy'}$ are zero but in practice this condition is never completely realized, both on

account of measurement noise and the fact that no geophysical structure is ever exactly two-dimensional. As interpretation procedures are only available at present for two-dimensional structures, a measure of two-dimensionality such as by the skew parameter (Swift 1967) where

$$\text{skew} = |Z_{xx} + Z_{yy}|/|Z_{xy} - Z_{yx}|$$

is required prior to interpretation. Skew is independent of the measuring axes and should be zero in a perfectly two-dimensional situation, but is normally accepted as indicative of two-dimensionality for the purpose of interpretation if its value is less than 0.4. When this condition is satisfied, it is possible to determine (a) the azimuth θ_0 of the principal impedance axis by maximizing

$$\{|Z_{xy'}(\theta)|^2 + |Z_{yx'}(\theta)|^2\}$$

(b) the principal impedances by substitution of θ_0 for θ in expressions for the tensor elements, and (c) the apparent resistivity values using equation (4). These principal apparent resistivities can be interpreted using one of the two-dimensional numerical methods such as that of Jones & Price (1969) in combination with an iterative programme for applying changes to the model to obtain a best-fit solution. In practice, the number of calculations is frequently prohibitive when considered in relation to the significance of the final model. As a result, two-dimensional methods are used in this study only in a semi-quantitative manner.

8 One-dimensional modelling

8.1 OL JORO OROK

Principal resistivity data for Ol Joro Orok (JOR) -- Fig. 5 – are less scattered and display a smaller degree of anisotropy than those for any other station, and are thus most suitable for a one-dimensional interpretation. The ρ_{max} curve is the one selected for this interpretation, since, as shown in Section 2, it corresponds to the E polarization curve, and can be expected to bear a closer relationship to the actual resistivities than the ρ_{min} curve.

The simplest quantitative deduction, obtained from the data by application of the 'method of asymptotes' to a two-layer model consisting of a lower layer which is much more conducting than the overburden, is that the top of the conductor lies less than 8 km under JOR. This estimate of the depth of the conductor d where

$$d = 0.8(\rho_a/\omega)^{1/2}\text{km}$$

(Keller & Frischknecht 1966, p. 223) is based on the apparent resistivity values only. Schmucker's inversion technique however uses both resistivity and phase information – see Section 7.4 – and this places more severe limits on the value of d.

The results of the application of this technique to both the maximum and minimum impedance data from JOR using equations (5) and (6) are illustrated in Figs. 9(a) and (b). They indicate a uniform conductor ($\sigma \sim 10^{-1}\,\text{S m}^{-1}$) extending from the surface to depths of more than 20 km.

The depth to the top of this uniform conductor can be independently estimated for each frequency component using equation (6). Estimates are plotted in Figs. 10(a) and (b) and show that the top of the conductor coincides with the earth's surface, within the limits of experimental accuracy.

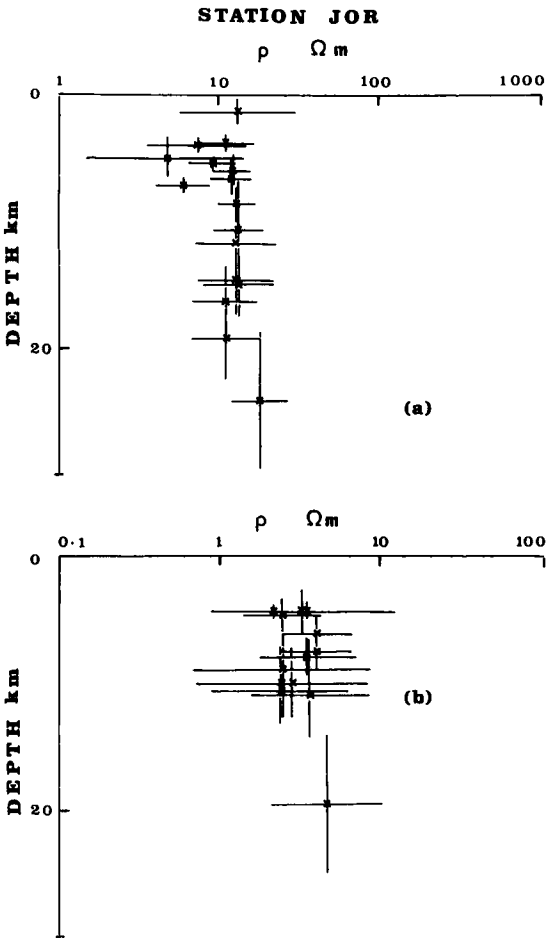

Figure 9. Schmucker inversion of the apparent resistivity data at JOR. (a) Maximum apparent resistivities. (b) Minimum apparent resistivities.

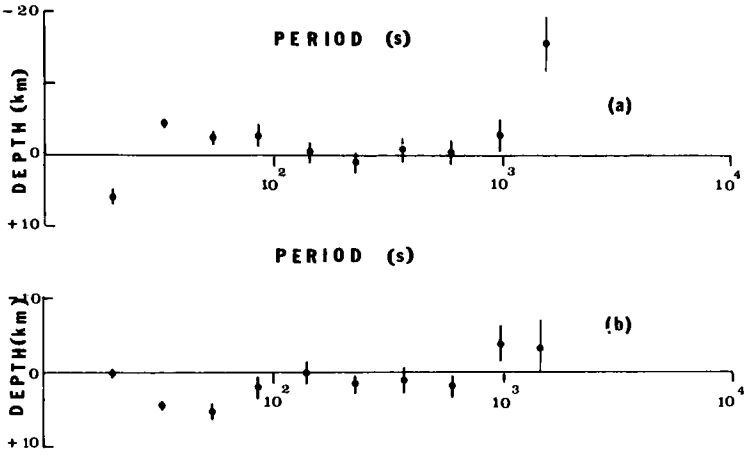

Figure 10. Depth to the top of a uniform conductor ($\sigma \sim 10^{-1}$ S m^{-1}) for: (a) maximum impedance data, (b) minimum impedance data.

The curve-fitting technique mentioned in Section 7.4 for layered media can also be applied to the JOR data. For two-layer master curves, the JOR E polarization resistivity curves can be fitted by a model consisting of a conductor overlying a resistor with a conductivity contrast of x 10 or more only if the conductor has a minimum thickness of 35 km. It is also possible to fit the JOR data within the error bars by a three-layer model consisting of a surface conductor and a deep conductor both of conductivity 10^{-1} S m^{-1} with a resistive layer ($\sigma < 10^{-2}$ S m^{-1}) between them. However, for a 5 km thickness of the surface conductor the top of the deep conductor can not lie more than 15 km below the surface.

It can thus be concluded that a one-dimensional interpretation of the ρ_{max} curve at JOR indicates the existence of a uniform conducting layer extending from the surface to a depth of more than 35 km. The data can not however resolve the existence of a 5–10 km thick resistant layer at a depth of more than 5 km.

8.2 MARIGAT

Marigat is the only rift valley station for which apparent resistivity data show a considerable frequency dependence. It was noted that the E and H polarization curves at MAR were very similar in shape to those obtained by Reddy & Rankin (1972) for a two-dimensional model corresponding to a sedimentary section 20 km wide and 1 km thick of resistivity 10 Ωm and surrounded on all sides by 1000 Ωm. Reddy & Rankin showed that the E polarization curve in this case is close to the one-dimensional curve at all periods. On this account it was considered justifiable to proceed with the curve-fitting technique to the MAR E polarization data. Fig. 11 shows the agreement between observed ρ_a and phase data and values computed for a model consisting of a top layer of 2 Ωm resistivity and 1 km thickness overlying a uniform conductor of resistivity 15 Ωm, a value which corresponds with that of ρ_{max} at the shortest periods at other rift valley stations.

It is interesting to note here that MAR lies between Lake Baringo and Lake Hannington and on top of lake sediments. An obvious interpretation of the Marigat resistivities is that they represent the inductive response of a shallow highly conducting sedimentary basin superimposed upon a uniform conducting layer below the rift.

Previous geophysical investigations using Schlumberger and electromagnetic soundings have determined the resistivity of the surface layer near Lake Hannington to be between 1 and 5 Ωm with a minimum thickness of 500 m (Harthill 1975, private communication). The consistency of the M–T and conventional resistivity data is gratifying.

9 Two-dimensional modelling

9.1 INTRODUCTION

The Pascoe–Jones (1971) finite difference program in its modified form (Jones & Thomson 1974) was used to calculate apparent resistivities for the two-dimensional conductor models of the Gregory Rift. The problems which arise in the use of this program are discussed fully by Rooney (1976). They are mainly associated with the choice of grid size and convergence criterion. While Muller & Losecke's (1975) method of continuing the iterations until the deviations at the end of each group of 50 iteration passes reach zero or oscillate only slightly around zero would doubtless have provided results of high reliability, the computational costs involved in its adoption for this project would have been prohibitive. For this reason, the less reliable convergence criterion, that a deviation of 0.01 per cent between iterative passes was assumed to indicate convergence, was used in the model fitting of the Kenyan data and the model results were used only as qualitative support of the results

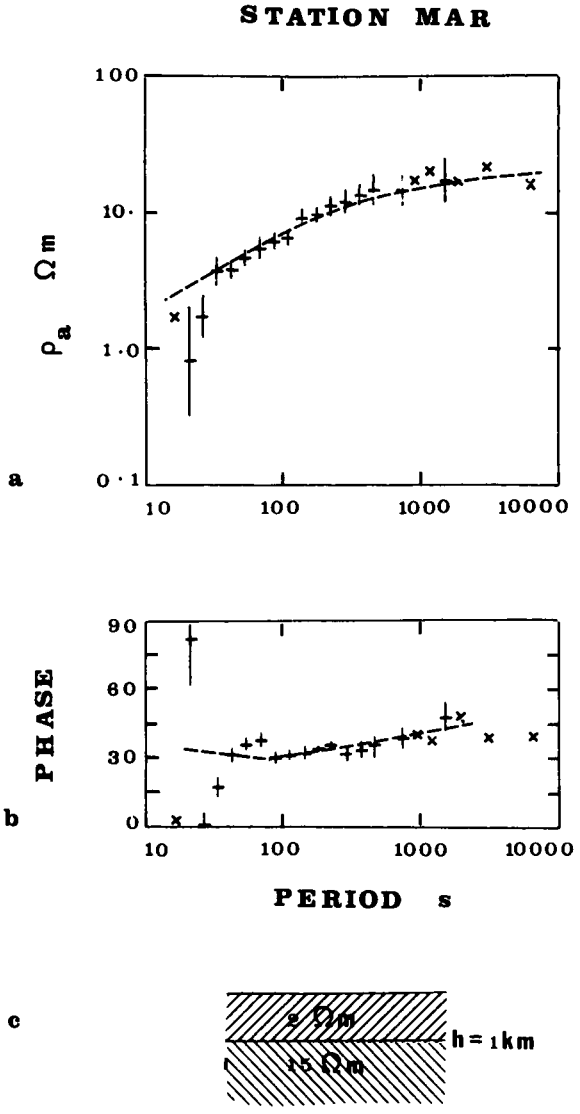

Figure 11. A two-layered interpretation of the maximum apparent resistivities at MAR. (a) Observed and model apparent resistivity curves. (b) Observed and model phase curves. (c) Two-layered model used in the computations.

of the one-dimensional M–T interpretation. On the basis of Muller & Losecke's investigation it would appear that Pascoe & Jones' convergence criterion is probably quite adequate to define the general form of the two-dimensional apparent resistivity curves and the correct value of resistivity to within better than 50 per cent of its 'true' value.

9.2 THE TWO-DIMENSIONAL MODELS

The primary concern of this interpretation is a determination of the geophysical nature of the conducting material below the rift. In particular, it is desired to use the magnetotelluric data in such a way as to discriminate between conductor models corresponding to (a) a

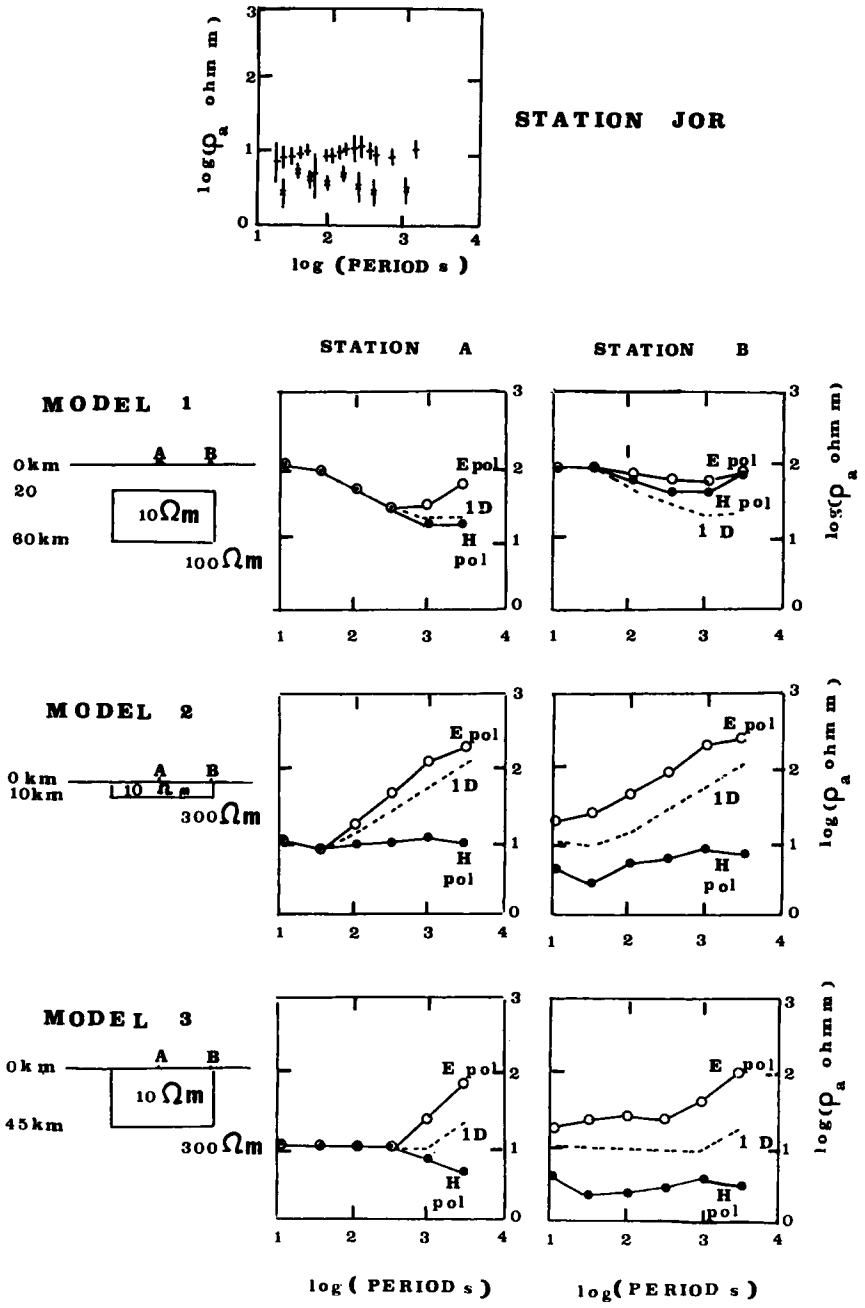

Figure 12. (a) Major and minor apparent resistivity versus period curves for JOR. (b)–(d) Computed one and two-dimensional apparent resistivity versus period curves for the earth models shown.

conductive infill of the rift (b) a conducting upper mantle and (c) a conductor confined entirely to the crust below the rift. Further elaboration of the conductive structure below the rift is left for future studies.

Even the simplest two-dimensional model considered here, consisting of a conductor of rectangular cross-section immersed in a resistive medium, is characterized by five in-

dependent parameters – (a) the width, (b) the depth to the top of the conductor, (c) its thickness, (d) the resistivity of the conductor and (e) the resistivity of the surrounding medium. An attempt to fit model and measured responses for a single rift station adds a sixth variable parameter, the station location, to the interpretation. Of these six parameters, (b) and (c) are the most interesting.

On the basis of the data and its qualitative interpretation, it seemed to be reasonable to assume that a value of 10 Ωm for the resistivity of the conductor and a width of 80 km would not lead to a loss in generality of the conclusions of subsequent two-dimensional interpretations. A reduction in width of the conductor to 60 km was, in fact, examined for several conductivity models and found to produce only a contraction in the horizontal scale of the model results. It was found, in addition, that the main findings of the modelling studies were not affected significantly by the value assigned to the resistivity of the surrounding medium, provided that this value was greater than 100 Ω m.

Fig. 12 illustrates the *E* polarization, *H* polarization and one-dimensional apparent resistivity curves calculated at two stations above three different conductivity distributions. Both stations lie above the conductor, with stations *A* and *B* located at distances of 40 and 2 km, respectively, from the lateral discontinuity. The three models shown in the figure are examples of upper mantle, surface and crustal conductors. Apparent resistivity data for station JOR are reproduced in Fig. 12(a) for the purpose of comparing the gross features of the model resistivity with the measured resistivities.

In discussing the model results, it is desirable not only to compare calculated and observed resistivities, but also to search for relationships between the two-dimensional curves and the equivalent one-dimensional curve. The latter involves fewer variables and it is thus more easily manipulated. Also it provides information relating solely to the depth distribution of conductivity, which is the primary interest of this study.

Model 1, (Fig. 12(b)), represents a good conductor in the upper mantle below the rift. For this model both *E* and *H* polarization curves lie close to the one-dimensional curve for periods less than 100 s, irrespective of the location of the station with respect to the lateral discontinuity. Even when the ambient medium has the very low resistivity of 100 Ω m, apparent resistivities at periods less than 100 s are one order of magnitude higher than those observed at the rift valley stations. In fact, there is reason to believe from a qualitative interpretation of the traverse data that JOR and MOL are near the edge of the conductor; the results at station *B* indicate that this would only increase the discrepancy between observed and calculated resistivities. It should be noted that for such a model, since the *E* polarization or ρ_{max} curve lies above the one-dimensional curve at all stations, an estimate of the maximum depth to the conductor based on the method of asymptotes is biased upwards. It follows that a conductor in the upper mantle beginning at just 20 km below the rift, can not *by itself* fit even the gross features of the rift valley data.

Principal resistivity curves calculated for the surface conductor, MODEL 2, Fig. 12(c), are quite similar in their frequency dependence to the resistivities measured at MAR, but are quite unlike those measured at rift stations lying on the line of traverse. *H* polarization resistivities show low, frequency-independent values similar to those observed at JOR. However, comparison of *H* polarization and one-dimensional curves at stations *A* and *B* shows that *H* polarization values are reacting very strongly to lateral changes of conductivity and can not be used to infer the depth distribution of conductivity. In contrast, the ρ_{max} curve appears to be strongly dependent on vertical conductivity changes and relatively little affected by lateral structure.

For this type of model, then, a one-dimensional interpretation of the ρ_{max} curve can be expected to give a good approximation to the actual conductivity variation with depth. This finding confirms the validity of a one-dimensional interpretation of the ρ_{max} data for

MAR, and also demonstrates the inadequacy of such a model to fit the long-period ρ_{max} values at other rift stations.

The final set of model results depicted in Fig. 12(d) was obtained for a very much thicker conductor extending downwards from the rift surface. It can be seen at once that the one-dimensional curve would give an acceptable fit to the ρ_{max} data at JOR. E polarization curves at stations more than 2 km from the discontinuity fit the ρ_{max} data reasonably well in magnitude and frequency dependence. Data published by Jones (1971) for two-dimensional conductors with different interface geometries suggest that the discrepancy between the E polarization and one-dimensional curves of MODEL 3 could be reduced by introducing a more gradual lateral conductivity change in place of the vertical discontinuity imposed by the modelling procedure. However, it is a common feature of all Jones' models that, independent of the nature of the lateral conductivity change, the E polarization curve always lies above the one-dimensional curve. A one-dimensional interpretation of the E polarization curve would give a slight underestimate of the conductivity and thickness of the conductor underlying the station. Following from the discussion of Section 8.1, it is clear that a conductor extending from the surface of the rift valley would provide a fit to the JOR ρ_{max} data only if its thickness exceeded 35 km. A conductor located entirely in the crust beneath the rift is insufficient to account for the low ρ_{max} values measured at long periods.

After considering single conductor models, computations were made for twin-conductor models corresponding to combinations of a surface conductor of resistivity 10 Ωm and a deep conductor, thickness 40 km and resistivity 10 Ωm, both immersed in a medium of resistivity 300 Ωm. For this type of model, apparent resistivities and induction responses tending to the form and magnitude of those at JOR and MOL could be found but only when the surface conductor was more than 5 km thick and the top surface of the deep conductor was less than 20 km beneath the rift floor.

Comparison of observed induction responses with those calculated for the three types of model confirms in general the deductions made above from the comparison of observed and computed resistivities. The computed induction responses are frequency independent – as observed – only for models of the third type.

10 Summary of the results of the modelling studies

The results of the modelling studies may be summarized as follows:

(i) Neither a surface conductor (<10 km thick) alone nor a single conductor at upper mantle depths (>15 km) can fit the apparent resistivity data or the frequency behaviour of the induction response data.

(ii) A composite model consisting of a conductor at 20 km depth representing conducting mantle and a surface conductor representing conductive infill of the rift cannot satisfy the M–T data unless the surface conductor is more than 5 km thick. Geological evidence (McCall 1967) suggests that the thickness of the rift infill is nowhere greater than 2–3 km and on the rift shoulders at MOL and JOR is much less.

(iii) The M–T data are broadly consistent with a model of high conductivity extending from the surface to depths of more than 35 km.

The data are not sufficient to resolve the presence of a resistive zone 5 km thick near the surface or 10–15 km thick at a depth below 5–10 km, but are sufficient to indicate the presence of a highly conducting zone in the upper crust (0–15 km) which cannot be explained in terms of a conductive infill of the rift. The M–T data can only be fitted by a model which also involves high conductivities at depths greater than 35 km, i.e. in the

upper mantle, but the vertical extent of this mantle conductor cannot be resolved. This conductivity model is similar to those which fit the M–T results obtained in Iceland (Hermance 1973) and in the Afar region of Ethiopia (Berktold 1974). Resistivities of 30 Ωm and 10 Ωm extending from depths of less than 5 km down to upper mantle depths have been proposed by Hermance and Berktold respectively for these regions.

11 Geophysical significance of the conductivity model

The most probable explanation of high conductivities in the upper mantle under the rift valley is the effect of partial melting caused by enhanced temperatures under the rift. The conductivity–temperature data published by Duba, Heard & Schock (1974) suggest that temperatures high enough to produce resistivities of the order of 10–25 Ωm in olivine are probably sufficiently high to induce partial melting of mantle material at these shallow depths (< 50 km) particularly if the mantle is wet (Wyllie 1971). Waff (1974) has estimated that for a mantle with a melt fraction C and a melt conductivity σ, the bulk mantle conductivity is $\frac{2}{3}C\sigma$. Using this expression and assuming a value of 3 S m^{-1} for the conductivity of basalt, it can be calculated that a partial melt fraction of less than 5 per cent is sufficient to produce a bulk resistivity of 10 Ωm in a mantle material composed predominantly of olivine.

The high conductivity also present at upper crustal depths in the Gregory Rift cannot reasonably be caused by (a) solid conduction in dry rocks, since the conductivity is too high, (b) basement mineralization since the volume would be excessive or (c) partial melting since temperatures of over 700°C would be required at depths of a few km. The only reasonable explanation for high conductivity in such a large volume of upper crustal rock is the presence of electrolytic fluids in the rock pores and fissures.

Moreover, a large temperature gradient (~ 60°C/km) has been found to be capable of reducing the resistivity of saturated rocks by up to one order of magnitude with a minimum of the order of 10 Ωm at depths of about 4 km (Hermance 1973). Also assuming a temperature gradient of 60°C/km, it follows from Lebedev & Khitarov's (1964) data for the electrical conductivity of granite as a function of temperature and water pressure and Hermance's calculation of water pressure versus depth, for such a temperature gradient, that water pressures at depths of more than 10 km are sufficient to lower the resistivity of granite to below 10 Ωm. Thus assuming that rocks of similar composition to granite will also display high conductivity under high water vapour pressures, it can be concluded that the high conductivities within the crust under the rift valley require large amounts of water to be present in the crust and high geothermal gradients. These conditions are, at the same time, consistent with the existence of a region of partial melting in the upper mantle below the Kenyan rift valley.

12 Conclusions

As the conclusions of previous geomagnetic deep sounding studies of this region (Banks & Ottey 1974; Beamish 1976) were heavily dependent upon other geophysical and geological data, this magnetotelluric study has for the first time provided independent evidence for the existence of high conductivities at depths corresponding to the upper mantle below the Kenyan rift valley. The explanation of this upper mantle conductor in terms of partial melting is in accord with geological evidence of recent volcanic activity in the area (Baker & Wohlenberg 1971) and with the mantle models suggested by Long & Backhouse (1976) to explain their data from the seismic array station at Kaptagat and by Fairhead (1976) to explain the regional gravity anomaly in Kenya.

The high conductivity also found at upper crustal depths can only reasonably be explained in terms of high temperatures and water saturation of the crust under the rift valley. This good conductor at depths less than 10 km prevents the resolution by the $M-T$ data of the depth to the top of and the thickness of the upper mantle conductor.

The possible existence of large quantities of water in the crust below the Gregory Rift and in the Sub-Icelandic and Sub-Ethiopian crusts suggests a relationship between high water concentration, high temperature and tectonic activity. The presence of water in rocks at high temperatures is also of considerable interest in the understanding of the petrology of rocks in the region of the rift valley.

Further wide-band magnetotelluric and accompanying geomagnetic deep sounding studies at other latitudes across, and to the south of, the great Rift Valley of East Africa would determine the degree of continuity of the crustal and upper mantle conductors along the axis of the rift and check the validity of the de Beer, Gough & van Zijl (1975) hypothesis that the rift conductor extends south-west to Botswana and South-west Africa. They would also contribute significantly to our understanding of the association of electrical conductivity structure and tectonic processes (Hutton 1977).

Acknowledgments

The authors wish to acknowledge the financial support of the Royal Society of London and the University of Edinburgh for the purchase of the instrumentation for the project and the fieldwork expenses. The Natural Environment Research Council, the Leverhulme Trustees and Edinburgh University provided studentships to one of us (DR) at various stages of this work. The magnetotelluric system was designed and built by Mr Ian M. Brazier. They are also indebted to him, to Mr Alex Jackson and others for invaluable assistance at the early stages of the fieldwork. Thanks are due also to the Government of Kenya for permission to work in their country and to the many Kenyans who provided facilities necessary for the observations and much warm hospitality. Professor N. J. Skinner and members of the Physics Department of the University of Nairobi provided generous facilities in their laboratories and many local problems were resolved with their assistance. Dr D. I. Gough is thanked for his helpful comments on the manuscript and for the assistance of the Institute of Earth and Planetary Physics, University of Alberta where the first draft was prepared.

Reterences

Albouy, Y., Godivier, R. & Perichon, P., 1971. Le sondage magnetotellurique, *ORSTOM publication*, Paris.

Baker, B. H., Mohr, P. A. & Williams, L. A., 1972. Geology of the Eastern Rift System of Africa, *Geol. Soc. Am. Sp. Paper 136*, 67 pp.

Baker, B. H. & Wohlenberg, J., 1971. Structure and evolution of the Kenya Rift Valley, *Nature*, **229**, 538–542.

Banks, R. J., 1973. Data processing and interpretation in geomagnetic deep sounding, *Phys. Earth planet. Int.*, 7, 339–348.

Banks, R. J. & Ottey, P., 1974. Geomagnetic Deep Sounding in and around the Kenya Rift Valley, *Geophys. J. R. astr. Soc.*, **36**, 321–335.

Beamish, D., 1976. A geomagnetic Deep Sounding Array Study of East Africa, *PhD thesis, University of Lancaster.*

Bentley, C. R., 1973. Error estimation in two-dimensional magnetotelluric analyses, *Phys. Earth planet. Int.*, 7, 423–430.

Berdichevsky, M. N., 1968. Electrical prospecting by the magnetotelluric profiling method, *Nedra*, Moscow.

Berktold, A., 1974. Ergebnisse der Magnetotellurik – messungen in Athiopien, *Protokoll uber das kolloquium erdmagnetische tiefensondierung, Grafath/Bayern*, **11**, 128–150.

Cagniard, L., 1953. Basic theory of the magnetotelluric method of geophysical prospecting, *Geophys.*, **18**, 605–635.

Caner, B. & Auld, D. R., 1968. Magnetotelluric determination of upper mantle conductivity structure at Victoria, British Columbia, *Can. J. Earth Sci.*, **5**, 1209–1220.

Coggon, J. H., 1971. *PhD thesis, University of California,* Berkeley, California.

de Beer, J. H., Gough, D. I. & van Zijl, J. S. O., 1975. An electrical conductivity Anomaly and Rifting in southern Africa, *Nature*, **225**, 678–680.

Dowling, F. L., 1970. Magnetotelluric measurements across the Wisconsin Arch, *J. geophys. Res.*, **75**, 2683–2698.

Duba, A., Heard, H. C. & Schock, R. N., 1974. Electrical conductivity of olivine at high pressure and under controlled oxygen fugacity, *J. geophys. Res.*, **79**, 1667–1673.

Fairhead, J. D., 1976. The structure of the lithosphere beneath the Eastern Rift, East Africa, deduced from gravity studies, *Tectonophys.*, **30**, 269–298.

Fairhead, J. D. & Girdler, R. W., 1972. The seismicity of the East African rift system, *Tectonophys.*, **15**, 115–122.

Fowler, R. A., Kotick, B. J. & Elliott, R. D., 1967. Polarisation analysis of natural and artificially induced geomagnetic micropulsations, *J. geophys. Res.*, **72**, 2871–2883.

Gough, D. I., 1973. The interpretation of magnetometer array studies, *Geophys. J. R. astr. Soc.*, **35**, 83–98.

Hermance, J. F., 1973. An electrical model for the Sub-Icelandic Crust, *Geophys.*, **38**, 3–13.

Hutton, Rosemary, 1972. Some problems of electromagnetic induction in the equatorial electrojet region. 1. Magnetotelluric relations, *Geophys. J. R. astr. Soc.*, **28**, 267–284.

Hutton, V. R. S., 1976. The electrical conductivity of the earth and planets, *Rep. Prog. Phys.*, **39**, 487–572.

Hutton, Rosemary, 1977. Induction studies in rifts and other active zones, *Acta Geod. Geoph. et Mont.*, in press.

Jolivet, I., 1966. *PhD thesis, University of Paris.*

Jones, F. W., 1971. Electromagnetic induction in a non-horizontally stratified two-layered conductor, *Geophys. J. R. astr. Soc.*, **22**, 17–28.

Jones, F. W. & Price, A. T., 1969. *IAGA Bulletin*, **26**, 196, Abstract 111–106.

Jones, F. W. & Price, A. T., 1970. The perturbation of alternating geomagnetic fields by conductivity anomalies, *Geophys. J. R. astr. Soc.*, **20**, 317–334.

Jones, F. W. & Thomson, D. J., 1974. A discussion of the finite difference method in computer modelling of electrical conductivity structure. A reply to the discussion by Williamson, Hewlett and Tammemagi, *Geophys. J. R. astr. Soc.*, **37**, 537.

Kanasewich, E. R., 1973. *Time sequence analysis in geophysics,* pp. 352, University of Alberta Press, Edmonton.

Keller, G. V. & Frischknecht, F. C., 1966. *Electrical methods in geophysical prospecting,* pp. 519, Pergamon Press, Oxford.

Knopoff, L. & Schlue, J. W., 1972. Rayleigh wave phase velocities for the path Addis Ababa–Nairobi, *Tectonophys.*, **15**, 157–163.

Kurtz, R. D. & Garland, G. D., 1976. Magnetotelluric measurements in eastern Canada, *Geophys. J. R. astr. Soc.*, **45**, 321–347.

Laird, C. E. & Bostick, F. X., 1970. One dimensional magnetotelluric inversion techniques, *Technical Report No. 101,* Electronics Research Centre, University of Texas, Austin, Texas.

Lebedev, E. B. & Khitarov, N. T., 1964. Dependence of the beginning of melting of granite and the electrical conductivity of its melt on high vapour pressure, *Geochem. Int.*, **1**, 193–197.

Long, R. E. & Backhouse, R. W., 1976. The structure of the Western Flank of the Gregory Rift Part II The Mantle, *Geophys. J. R. astr. Soc.*, **44**, 677–688.

McCall, G. J. H., 1967. Geology of the Nakuru–Thomson's Falls – Lake Hannington area, *Geol. Survey, Kenya, Rep. 78.*

Madden, T. R. & Swift, C. M., 1969. Magnetotelluric studies of electrical conductivity structure of the crust and upper mantle in *The earth crust and upper mantle,* ed. P. H. Hart, *Geophys. Monogr.*, **13**, 469–479, Am. geophys. Un.

Milanovsky, E. E., 1972. Continental rift zones: their arrangement and development, *Tectonophys.*, **15**, 65–70.

Muller, W. & Losecke, W., 1975. Accelerating convergence techniques and grid spacing problems in two-dimensional magnetotelluric modelling, *Geophys. J. R. astr. Soc.*, **41**, 185–191.

Neinaber, W., Auld, D. R. & Dosso, H. W., 1973. Analysis of anisotropic magnetotelluric measurements at Victoria, B.C., *Can. J. Earth Sci.*, **10**, 557–570.

O'Connell, R. B., 1972. Geological development of the rift system of Eastern Africa, *Geol. Soc. Am. Bull.*, **83**, 2549–2572.

Pascoe, L. J. & Jones, F. W., 1971. Boundary conditions and calculation of surface values for the general two-dimensional electromagnetic induction problem, *Geophys. J. R. astr. Soc.*, **27**, 179–193.

Porstendorfer, G., 1975. *Principles of magneto-telluric prospecting, Geoexploration Monographs Series 1*, No. 5, p. 118, eds Kunetz, G. & Parasnis, D. S., Gebrüder Borntraeger–Berlin West and Stuttgart.

Price, A. T., 1962. The theory of magnetotelluric methods when the source field is considered, *J. geophys. Res.*, **67**, 1907–1918.

Reddy, T. K. & Rankin, D., 1972. On the interpretation of magnetotelluric data in the Plains of Alberta, *Can. J. Earth Sci.*, **9**, 514–527.

Reitmayr, G., 1975. An anomaly of the upper mantle below the Rhinegraben studied by the inductive response of natural electromagnetic fields, *J. Geophys.*, **41**, 651–658.

Rooney, D., 1976. Magnetotelluric measurements across the Kenyan Rift Valley, *PhD thesis, University of Edinburgh.*

Schmucker, U., 1970. Analysis of geomagnetic variations in the Southwestern United States, *Bull. Scripps Inst. Oceanogr.*, **13**, pp. 165, University of California, San Diego.

Schmucker, U., 1973. Regional induction studies: a review of methods and results, *Phys. Earth planet. Int.*, **7**, 365–378.

Scholtz, C. H., Koczynski, T. A. & Hutchins, D. G., 1976. Evidence for incipient rifting in Southern Africa, *Geophys. J. R. astr. Soc.*, **44**, 135–144.

Sims, W. E. & Bostick, F. X., 1969. Methods of magnetotelluric analysis, *EGRL Tech. Report 58*, University of Texas, Austin.

Sims, W. E., Bostick, F. X. & Smith, H. W., 1971. The estimation of magnetotelluric impedance tensor elements from measured data, *Geophys.*, **36**, 938–942.

Swift, C. M., 1967. *PhD thesis, University of Toronto.*

Trigg, D. F., Serson, P. H. & Camfield, P. A., 1970. A solid state electrical recording magnetometer, *Publ. Earth Phys. Branch*, **41**, No. 5, Ottawa.

Vozoff, K., 1972. The magnetotelluric method in the exploration of sedimentary basins, *Geophys.*, **37**, 98–141.

Waff, H. S., 1974. Theoretical considerations of electrical conductivity in a partially molten mantle and implications for geothermometry, *J. geophys. Res.*, **79**, 4003–4010.

Weidelt, P., 1972. The inverse problem of geomagnetic induction, *Z. Geophys.*, **38**, 257–289.

Wyllie, P. J., 1971. Role of water in magma generation and initiation of diapiric uprise in the mantle, *J. geophys. Res.*, **76**, 1328–1338.